Eur. J. Biochem. 222, 441–447 (1994)

Stability and structural analysis of α-amylase from the antarctic psychrophile *Alteromonas haloplanctis* A23

Georges FELLER[1], Françoise PAYAN[2], Fabienne THEYS[1], Minxie QIAN[2], Richard HASER[2] and Charles GERDAY[1]

[1] Laboratory of Biochemistry, Institute of Chemistry B6, University of Liège, Belgium
[2] Laboratoire de Cristallographie et Cristallisation des Macromolecules Biologiques, Centre National de la Recherche Scientifique, Faculté de Médecine Nord, Marseille, France

(Received February 14/March 21, 1994) – EJB 94 0202/3

The α-amylase secreted by the antarctic bacterium *Alteromonas haloplanctis* displays 66% amino acid sequence similarity with porcine pancreatic α-amylase. The psychrophilic α-amylase is however characterized by a sevenfold higher k_{cat} and k_{cat}/K_m values at 4°C and a lower conformational stability estimated as 10 kJ · mol^{-1} with respect to the porcine enzyme. It is proposed that both properties arise from an increase in molecular flexibility required to compensate for the reduction of reaction rates at low temperatures. This is supported by the fast denaturation rates induced by temperature, urea or guanidinium chloride and by the shift towards low temperatures of the apparent optimal temperature of activity.

When compared with the known three-dimensional structure of porcine pancreatic α-amylase, homology modelling of the psychrophilic α-amylase reveals several features which may be assumed to be responsible for a more flexible, heat-labile conformation: the lack of several surface salt bridges in the $(\beta/\alpha)_8$ domain, the reduction of the number of weakly polar interactions involving an aromatic side chain, a lower hydrophobicity associated with the increased flexibility index of amino acids forming the hydrophobic clusters and by substitutions of proline for alanine residues in loops connecting secondary structures. The weaker affinity of the enzyme for Ca^{2+} (K_d = 44 nM) and for Cl^- (K_d = 1.2 mM at 4°C) can result from single amino acid substitutions in the Ca^{2+}-binding and Cl^--binding sites and can also affect the compactness of α-amylase.

The physical basis of the forces driving the folding of a polypeptide chain and maintaining the final structure remains only understood in general terms. Accordingly, the relative contributions of the determinants of protein stability, mainly the various weak electrostatic interactions and the hydrophobic effect, are still under debate (Creighton, 1991). Amongst the several approaches currently used, the analysis of proteins from extremophiles provides valuable insights on the molecular strategies adopted in response to environmental stress such as extremes of pH, pressure, salinity or temperature (Zuber, 1988; Jaenicke, 1991). Enzymes from thermophilic microorganisms for example seem stabilized by strengthening one or a combination of noncovalent interactions making use of a small number of amino acid replacements (Fontana, 1991; Jaenicke, 1991).

By contrast, psychrophilic microorganisms persisting at low temperatures have received little attention. Enzymes from these organisms are characterized by marked heat lability which has been commonly correlated with environmental conditions (Ushakov, 1964). However, enzymes from psychrophiles also display high specific activity which is the main property for enzyme adaptation to catalysis at low environmental temperatures. Hochachka and Somero (1984) have argued that enzymes which can readily undergo conformational changes during catalysis at low temperature are capable of supplying most of the energy for activation events and can reduce the activation energy barrier of their chemical reactions. Thermal instability is regarded as the consequence of the highly flexible structure of cold-active enzymes. Psychrophilic enzymes that have evolved towards high conformational flexibility and catalytic efficiency therefore represent appropriate candidates for protein-stability analysis. Cloning of genes from psychrophilic bacteria in *Escherichia coli* results in the expression of thermolabile recombinant enzymes active at temperatures close to 0°C demonstrating the intrinsic character of these properties (Feller et al., 1991; Davail et al., 1992; Rentier-Delrue et al., 1993). In most cases however, the analysis of psychrophilic protein sequences has been impaired by insufficient isology with their mesophilic counterparts.

We have previously reported the characterization and the nucleotide sequence of the α-amylase secreted by a Gram-negative antarctic bacterium *Alteromonas haloplanctis* (Feller et al., 1992). In this study, we report typical stability parameters of *A. haloplanctis* and porcine pancreatic α-amylases. A model of the heat labile α-amylase has been constructed on the basis of the three-dimensional structure of the porcine enzyme recently solved at 0.21-nm resolution (Qian et al., 1993).

Correspondence to G. Feller, Laboratory of Biochemistry, Institute of Chemistry B6, University of Liège, B-4000 Liège, Belgium
Fax: +32 41563364.

Abbreviations. Np(Glc*p*)$_7$OCH$_3$CH^{2+}, 4-nitrophenyl-α-D-maltoheptaoside-4,6-*O*-ethylidene; GdmCl, guanidinium chloride.

Enzymes. α-Amylase or 1,4-α-D-glucan glucanohydrolase (EC 3.2.1.1).

Table 1. Kinetic parameters for the amylolytic activity of *A. haloplanctis* and porcine pancreatic α-amylases. Linear reaction rates were recorded in 100 mM Hepes, 50 mM NaCl, 10 mM $MgCl_2$, pH 7.1. Assays using $Np(Glcp)_7OCH_3CH^{2+}$ as substrate also contained 23 U/ml α-glucosidase as coupling enzyme. Substrate concentrations were varied from $0.4-4 \times K_m$. k_{cat} values for starch are calculated on the basis of maltose released. Values are the mean of at least three determination sets. SE for k_{cat} and K_m was ≤5% [$Np(Glcp)_7OCH_3CH^{2+}$] and ≤8% (starch).

α-Amylase	Assay temperature	Substrate					
		starch			$Np(Glcp)_7OCH_3CH^{2+}$		
		k_{cat}	K_m	k_{cat}/K_m	k_{cat}	K_m	k_{cat}/K_m
	°C	s^{-1}	$g \cdot l^{-1}$	$s^{-1} \cdot g^{-1} \cdot l$	s^{-1}	μM	$s^{-1} \cdot \mu M^{-1}$
A. haloplanctis	4	490	1.09	450	233	820	0.28
	25	1363	1.27	1075	1504	186	8.08
Porcine	4	71	1.05	68	38	276	0.14
	25	326	1.12	292	394	87	4.54

MATERIALS AND METHODS

Sources

The heterotrophic aerobic strain *A. haloplanctis* A23 was isolated near the Dumont d'Urville antarctic station (60°40′ S, 40°01′E). Porcine pancreatic α-amylase was from Sigma (A6255).

Purification of *A. haloplanctis* α-amylase

The antarctic strain was cultivated at 4°C for 3 days in 3.5 l broth containing 10 g/l bactotryptone, 5 g/l yeast extract, 20 g/l NaCl, 10 g/l sea salts, 20 g/l maltose, pH 7.6, vigorously aerated by air bubbling. After centrifugation at 11000 *g*, the culture supernatant was adjusted to 0.02% NaN_3, concentrated to 400 ml and diafiltrated against 50 mM Tris/HCl, 1 mM $CaCl_2$, pH 7.5, using a Minitan tangential flow ultrafiltration unit (Millipore) fitted with PTGC membranes (10-kDa retention limit). The sample was loaded on a DEAE-agarose column (2.5 cm×40 cm) equilibrated in the above mentioned buffer and eluted with a NaCl linear gradient (500 ml each starting buffer, 0−0.8 M NaCl). Fractions containing amylolytic activity were concentrated to 10 ml and applied onto a Sephadex G-100 column (2.5 cm×100 cm) eluted with 50 mM Tris/HCl, 1 mM $CaCl_2$, pH 7.0, followed by gel filtration on an Ultrogel AcA 54 column (2.5 cm×100 cm) eluted with the same buffer. For further experiments, the purified α-amylases were conditioned in the appropriate buffers by gel filtration on a PD-10 column (Pharmacia).

Enzyme assay

The standard assay was carried out at 25°C with the α-amylase EPS kit (Boehringer) using 3.5 mM 4-nitrophenyl-α-D-maltoheptaoside-4,6-*O*-ethylidene [$Np(Glcp)_7OCH_3CH^{2+}$] as substrate and excess (23 U/ml) of α-glucosidase as coupling enzyme in 100 mM Hepes, 50 mM NaCl, 10 mM $MgCl_2$, pH 7.1. Activities towards the synthetic substrate were recorded in a thermostated Uvicon 860 spectrophotometer (Kontron) and values were calculated using an absorption coefficient for 4-nitrophenol of 8980 $M^{-1} \cdot cm^{-1}$ at 405 nm (Raucher et al., 1985). The amylolytic activity was also determined by the dinitrosalicylic acid method (Bernfeld, 1955) using 1% soluble starch (Sigma) as substrate in the above-mentioned buffer.

Analytical procedures

The enzyme concentrations were determined spectrophotometrically by using $A^{0.1\%} = 2.41$ at 280 nm for the porcine α-amylase (Levitzki and Steer, 1974) and $A^{0.1\%} = 1.90$ at 280 nm for the bacterial α-amylase. The kinetic parameters k_{cat} and K_m were determined by the initial velocity method using a nonlinear regression computer fit of the saturation curves.

Cl^--free α-amylase was prepared by gel filtration on a PD-10 column eluted with 25 mM Hepes/NaOH, pH 7.0. The dissociation constants for Cl^- were calculated from computer-fitted activation curves generated by NaCl titration in the above-mentioned reaction mixture except that the buffer was replaced by 25 mM Hepes/NaOH, pH 7.0. Apo α-amylase (Cl^-, Ca^{2+}-free) was prepared by overnight dialysis of the native enzyme against 25 mM Hepes/NaOH, 5 mM EGTA, pH 8.0. Activation kinetics obtained by calcium titration were performed in 25 mM Hepes/NaOH, 50 mM NaCl, 5 mM EGTA, 3.5 mM $Np(Glcp)_7OCH_3CH^{2+}$, 23 U/ml α-glucosidase, pH 8.0. The desired free Ca^{2+} concentration was set by addition of 50 mM $CaCl_2$ according to a program developed by Robertson et al. (1982). The data points were computer fitted according to the Hill equation.

Guanidinium chloride (GdmCl) denaturation curves were recorded according to Pace et al. (1989). Enzymes (36 μg/ml) were subjected to increasing GdmCl concentrations in 30 mM Mops, pH 7.0. Following 4 h incubation at 25°C, the fluorescence intensity of the samples was recorded using a Perkin Elmer LS 50 spectrofluorimeter at an excitation wavelength of 280 nm. Emission wavelengths were 340 nm and 347 nm for the porcine and *A. haloplanctis* α-amylases respectively.

Molecular modelling

The psychrophilic α-amylase model was constructed from the porcine pancreatic α-amylase coordinates using the program TURBO-FRODO (Roussel and Cambillau, 1990). Few insertions were operated and deletions mainly affected surface loops between Aβ3 and Bβ7, between Aα4 and Aβ5 and between Aβ8 and Aα8. Amino acid replacements were generated in the low energy conformation. Energy minimization and low-temperature molecular dynamics were carried out using X-PLOR (Brünger et al., 1987).

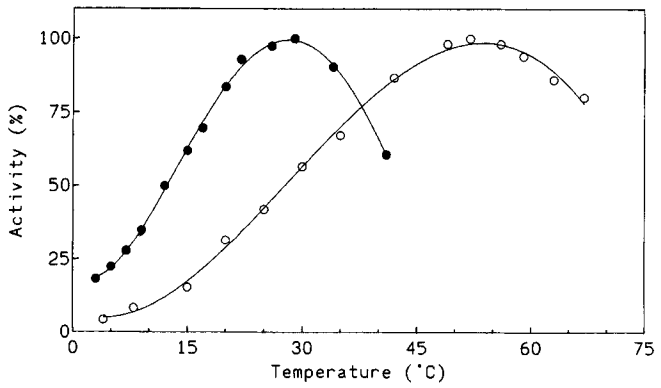

Fig. 1. Effect of assay temperature on amylolytic activity. Specific activities of *A. haloplanctis* (●) and porcine pancreatic (○) α-amylases were recorded at increasing temperatures using 3.5 mM $Np(Glcp)_7OCH_3CH^{2+}$ as substrate under standard assay conditions. Reaction rates are reported relative to the maximal activity recorded.

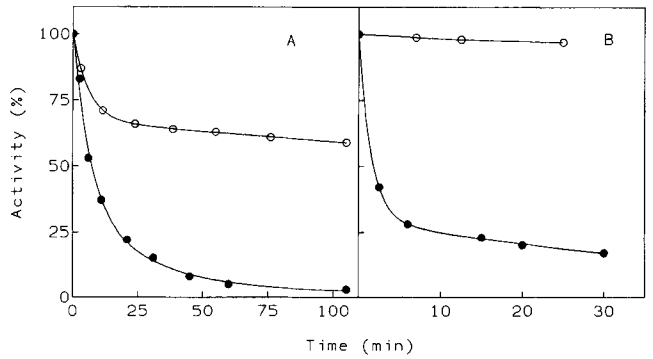

Fig. 2. Thermal stability (A) and urea denaturation (B) of the amylolytic activity. (A) *A. haloplanctis* (●) and porcine pancreatic (○) α-amylases were incubated at 50°C in 50 mM Tris/HCl, 1 mM $CaCl_2$, pH 7.0, and residual activities were recorded under standard assay conditions using 3.5 mM $Np(Glcp)_7OCH_3CH^{2+}$ as substrate. (B) *A. haloplanctis* and porcine pancreatic α-amylases (symbols as in A) were incubated at 25°C in the above mentioned buffer including 3.2 M urea and residual activities were recorded under standard assay conditions.

RESULTS

Thermodependence of enzyme activity

The kinetic parameters k_{cat}, K_m and the physiological efficiency k_{cat}/K_m for the amylolytic activity of the bacterial and the porcine α-amylases are given in Table 1. The k_{cat} of the psychrophilic α-amylase towards the natural substrate at 4°C is seven times the value displayed by the porcine enzyme. As a result of similar K_m values for starch in both enzymes, the k_{cat}/K_m ratio is also more favourable to *A. haloplanctis* α-amylase. The same behaviour is recorded using the synthetic substrate $Np(Glcp)_7OCH_3CH^{2+}$, although the Michaelis constants of *A. haloplanctis* α-amylase are larger. The thermodependencies of the amylolytic activity of both enzymes are shown in Fig. 1. The drastic shift of the apparent optimal temperature of activity (from 50°C for the porcine enzyme to 30°C for the bacterial enzyme) indicates that thermally induced alterations of the catalytic mechanism occur at moderate temperatures in the case of the psychrophilic α-amylase.

α-Amylase stability

The thermal stability of the amylolytic activity of both α-amylases is shown by the denaturation curves at 50°C (Fig. 2A). The half time of inactivation (t_i) for the *A. haloplanctis* protein is approximately 20 times lower than for the porcine α-amylase. The difference in free energy of stabilization between both enzymes, estimated by the relation $\Delta\Delta G = 2.3RT\log(t_{i1}/t_{i2})$, amounts to 8 kJ · mol^{-1}. As shown in Fig. 2B, urea also induces a very fast inactivation of *A. haloplanctis* α-amylase. The GdmCl denaturation curves of both α-amylases monitored by intrinsic fluorescence are shown in Fig. 3. As the denaturant concentration increases, the fraction of native porcine enzyme molecules decreases according to a biphasic decay; the transition step can arise from the unfolding of different domains. The concentration for half denaturation $[GdmCl]_{1/2}$ is 1.4 M. In the case of *A. haloplanctis* α-amylase, GdmCl induces a fast denaturation of the protein structure with a $[GdmCl]_{1/2}$ value of 0.8 M. The curve only displays a minor deviation corresponding to the transition step of the porcine protein indicative of a less accentuated resistance of the bacterial α-amylase structure to GdmCl. The difference in conformational stability between the psychrophilic and the porcine α-amylases has been estimated by the relation $\Delta\Delta G = \Delta([GdmCl]_{1/2})m_a$, where m_a is the average value of the slopes from plots of [GdmCl] versus the free energy of unfolding, $\Delta G_d = \Delta G_{H_2O} - m[GdmCl]$ (Pace et al., 1989). This difference in conformational stability amounts to 10 kJ · mol^{-1} and is in reasonable agreement with the thermal inactivation estimate.

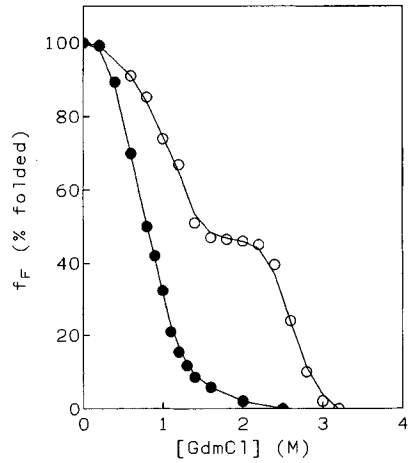

Fig. 3. Guanidinium-chloride-induced unfolding curves. The folded fraction f_F of *A. haloplanctis* (●) and porcine pancreatic (○) α-amylases is plotted for increasing GdmCl concentrations. Fluorescence intensities of α-amylases (36 μg/ml) were recorded at 25°C in 30 mM Mops, pH 7.0. The fraction of protein in the folded state f_F was calculated using $f_F = y - y_D/y_N - y_D$, where y_N and y_D are the fluorescence intensities of the native state and the fully denatured state respectively; y is the fluorescence intensity at a given GdmCl concentration.

Dissociation constants

Removal of either Ca^{2+} or Cl^- results in the reversible inactivation of *A. haloplanctis* α-amylase. This allows the determination of the dissociation constants, K_d, by activation kinetics following calcium or chloride titration. Fig. 4 shows the allosteric activation by these ions. The deduced K_d values are compared in Table 2 with those previously determined for the pancreatic α-amylase. The binding affinity for both ions is

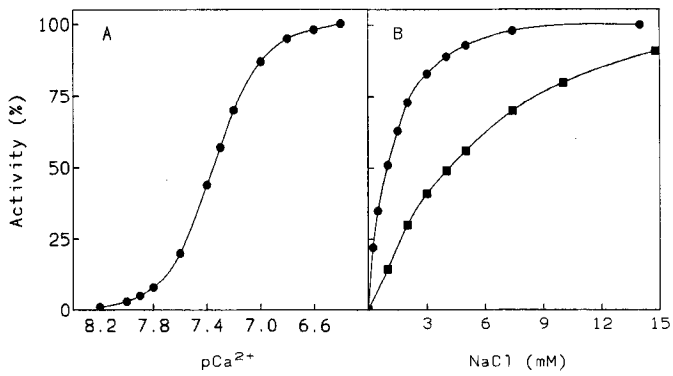

Fig. 4. Activation of *A. haloplanctis* α-amylase by Ca^{2+} and Cl^-. (A) Calcium titration of the Ca^{2+}-free enzyme in the presence of 5 mM EGTA and chloride; $pCa^{2+} = -\log[Ca^{2+}]$. (B) Chloride titration of the Cl^--free enzyme at 4°C (●) and 25°C (■).

Table 2. Dissociation constants of the Cl^--amylase and the Ca^{2+}/amylase complexes. K_d data from *A. haloplanctis* α-amylase are derived from activation kinetics experiments shown in Fig. 2. SE for K_d was ≤5% (Cl^-) and 12% (Ca^{2+}). K_d data for porcine pancreatic α-amylase are taken from Levitzki and Steer (1974).

α-Amylase	K_d		
	Cl^-		Ca^{2+}
	4 °C	25 °C	25 °C
	mM		nM
A. haloplanctis	1.2	6.7	44
Porcine	0.093	0.29	0.02

significantly lower in the psychophilic α-amylase as indicated by a 10−20-fold increase of the K_d value for Cl^- and a 2000-fold higher K_d-value for Ca^{2+}.

A. haloplanctis α-amylase structural model analysis

Amino acid sequences of *A. haloplanctis* and porcine pancreatic α-amylases can be aligned with 53% positional identity. This value increases to 66% when considering amino acid residues of the same type (Fig. 5). Conserved amino acids occur essentially in the secondary structures of the porcine enzyme and in regions bearing functional residues pertaining to the active site as well as to the ion-binding sites. This favourable degree of identity allowed the building of a model of the three-dimensional structure of the psychrophilic α-amylase. The predicted molecular architecture follows the pattern of known α-amylase structures (Swift et al., 1991; Qian et al., 1993). The enzyme is made of a central $(\beta/\alpha)_8$ barrel (domain A), a β-pleated domain B and a globular C-terminal domain C. Amino acids with their side chain directed towards the active site, amongst which Glu233, Asp300 and Asp197 are the main catalytic residues, are conserved suggesting a very close reaction mechanism in both enzymes. The structural model of *A. haloplanctis* α-amylase was analyzed in order to identify the weak interactions and the structural features potentially involved in the structure flexibility of the psychrophilic enzyme. The results are summarized in Table 3.

```
          10        20        30        40        50
********TPTTFVHLFEWNWQDVAQECEQYLGPKGYAAVQVSPPNEHI**T*GS
QYAPQTQSGRTSIVHLFEWRWVDIALECERYLGPKGFGGVQVSPPNENVVVTNPS
            Aß1             Aα1          Aß2a  Aß2b
   60        70        80        90       100       110
Q*WWTRYQPVSYELQSRGGNRAQFIDMVNRCSAAGVDIYVDTLINHM***AAGSG
RPWWERYQPVSYKLCTRSGNENEFRDMVTRCNNVGVRIYVDAVINHMCGSGAAAG
                          Aα2       Aß3     Bß1
        120       130       140       150       160
TGTAGNSFGN***KSFP*I*YSPQDFHES*C*T*INNSDYGNDRYRVQNCELVGL
TGTTCGSYCNPGSREFPAVPYSAWDFNDGKCKTASGGIESYNDPYQVRDCQLVGL
 Bß2     Bß3   Bß4   Bß5 Bß6        Bß7       Bα1   Bß8
   170       180       190       200       210       220
ADLDTASNYVQNTIAAYINDLQAIGVKGFRFDASKHVAASDIQSLMAK***VN**
LDLALEKDYVRSMIADYLNKLIDIGVAGFRIDASKHMWPGDIKAVLDKLHNLNTN
 Bß9           Aα3         Aß4         Aα4
        230       240       250       260       270
****GS*PVVFQEVIDQGGEAVGASEYLSTGLVTEFKYSTELGNTFRNGSLA***
WFPAGSRPFIFQEVIDLGGEAISSSEYFGNGRVTEFKYGAKLGTVVRKWSGEKMS
           Aß5          A3105   Aß6     Aα6a
   280       290       300       310       320
WLSNFGEGWGFMPSSSAVVFVDNHDNQRGHGGAGNVI*TFEDGRLYDLANVFMLA
YLKNWGEGWGFMPSDRALVFVDNHDNQRGHGAGGSSILTFWDARLYKVAVGFMLA
A3106b        Aß7                                 Aα7
        340       350       360       370       380
YPYGYPKVMSSYDFHGDTDAGGP*N**V*PVHNNG*******NLE**CFASNWKC
HPYGFTRVMSSYRWARNFVNGEDVNDWIGPPNNNGVIKEVTINADTTC*GNDWVC
     Aß8
   390       400       410       420       430
EHRWSYIAGGVDFRNNTADNWAVTNWWDNTNNQISFGRGSSGHMAINKEDSTLTA
EHRWREIRNMVWFRNV*VDGQPFANWWDNGSNQVAFGRGNRGFIVFNNDDWQLSS
          Aα8         Cß1       Cß2     Cß3
        450       460       470       480       490
TVQTDMASGQYCNVLKGELSADAKSCSGEVITVNSDGTINLNIG**AWDAM*AIH
TLQTGLPGGTYCDVISGDK*V*GNSCTGIKVYVSSDGTAQFSISNSAEDPFIAIH
Cß4       Cß5       Cß6   Cß7  Cß8       Cß9       Cß10

KNAKLNTSSAS 453 AHA
AESKL****** 496 PPA
```

Fig. 5. Amino acid sequence alignment of *A. haloplanctis* and porcine pancreatic α-amylases. Residues are numbered according to the porcine α-amylase sequence with no number for inserted residues and no number shift for deleted residues. The secondary structures of the porcine enzyme identified by Qian et al. (1993) are underlined; deleted or inserted residues are indicated (*). 238 amino acids of *A. haloplanctis* α-amylase are conserved in the porcine enzyme. When considering residues of the same type (G = A = S, S = T, L = I = V, F = W = Y, E = D = R = K, Q = N), 301 amino acid residues are conserved.

Disulfide bonds

A. haloplanctis α-amylase contains eight cysteine residues. Sulfhydryl titration by 5,5′-dithiobis-(2-nitrobenzoic acid) of both the native and the denatured enzyme in 8 M urea indicates that there is no free thiol group. Since the positions of these cysteine residues correspond to residues forming disulfide linkage in the porcine α-amylase, four conserved disulfide bonds are proposed for the bacterial enzyme (28−86, 141−160, 378−384, 450−462).

DISCUSSION

The k_{cat} and k_{cat}/K_m values of the α-amylase excreted by *A. haloplanctis* are larger than the values determined for the porcine enzyme over a temperature range of 0°C to at least 25°C. This increase largely compensates for the reduction of the reaction rates occurring at low temperatures since both k_{cat} and k_{cat}/K_m values for starch of the psychrophilic α-amylase at 4°C are higher than the corresponding values of the pancreatic

Table 3. Structural parameters potentially involved in the stability of α-amylase conformation. −, denotes an expected decrease of stability; (), low or undefined effect. ΣH_i, sum of the hydrophobicity values H_i from the PRIFT scale (Cornette et al., 1987) for the 25 substitutions in the hydrophobic clusters of *A. haloplanctis* and porcine pancreatic α-amylases.

Parameter	α-Amylase		Expected effect on stability
	A. haloplanctis	Porcine	
Salt bridges	7	19	−
Amino-aromatic interactions	9	20	−
Oxygen-aromatic interactions	13	19	−
Sulfur-aromatic interactions	2	5	−
Aromatic-aromatic interactions	19	20	0
Hydrophobic clusters (ΣH_i)	47	103	−
Proline content	13	21	−
Arginine content	13	29	−
Disulfide bonds	4	5	(0)
Helices dipoles − charges at Nα	2	4	(−)
Helices dipoles + charges at Cα	3	6	(−)
Ca^{2+} affinity	low	high	−
Cl^- affinity	low	high	−

enzyme at 25°C. Hochachka and Somero (1984) have proposed that this catalytic efficiency can be gained by an appropriate folding flexibility. A loose conformation of the psychrophilic α-amylase is indeed suggested by the susceptibility of secondary structures to unfolding at moderate temperatures (Feller et al., 1992), by the fast denaturation rates induced by temperature, urea or GdmCl and by the shift of the apparent optimal temperature of activity. The high dissociation constants for Ca^{2+} and Cl^- possibly also reflect a less compact protein structure.

Ca^{2+}-binding and Cl^--binding sites

Calcium coordination in porcine pancreatic α-amylase occurs through a pentagonal bipyramid involving the carboxyl oxygens of Asp167 and the carbonyl oxygen of His201 at the apices, three water molecules, $O^{\delta 1}$ of Asn100 and the main-chain carbonyl of Arg158. The latter is replaced by Gln158 in *A. haloplanctis* α-amylase whereas the other Ca^{2+} ligands are conserved. As Arg158 in the porcine enzyme coordinates the Ca^{2+} ion via the main-chain carbonyl, there is apparently no drastic modification of the *A. haloplanctis* α-amylase binding site that would account for its 2000 times lower binding affinity. In the porcine enzyme however, Arg158 forms a salt bridge with Glu246 and, as a result of its charge resonance structure, also forms an amino-aromatic interaction with Trp203 (alanine in *A. haloplanctis* α-amylase). The three residues are conserved in all mammalian α-amylases. As these interactions are absent in the bacterial enzyme, Gln158 is less firmly oriented in the Ca^{2+}-binding site. The Ca^{2+} of α-amylases bridges a cleft between domains A and B forming the active site (Qian et al., 1993). If the high specific activity of the psychrophilic α-amylase is a consequence of a more flexible active site, then the substitution Arg158→Gln is certainly of importance through its effect of weakening interdomain contacts around the catalytic cleft.

The chloride-binding site of the pancreatic α-amylase is composed by Arg195 ($N^{\eta 2}$), Asn298 ($N^{\delta 2}$) and the side-chain amine of Arg337 coordinating Cl^- in a bidentate mode. This chloride-binding site is conserved in all mammalian α-amylases but differs in *A. haloplanctis* by a lysine residue instead of Arg337. As lysine can only provide an unidentate coordination, this substitution can account for the 10−20-fold lower Cl^--binding affinity of the psychrophilic α-amylase.

Calcium protects α-amylases against heat inactivation (Vihinen and Mäntsälä, 1989) and we have found that chloride is required for optimal stability of *A. haloplanctis* α-amylase (Feller et al., 1992). It follows that the low Ca^{2+}-binding and Cl^--binding affinities are additional factors leading to a low stability. In thermophiles, stabilization by tight calcium binding is well documented and involves either unusual high affinity or even extra Ca^{2+}-binding sites (Teplyakov et al., 1990). No equivalent Cl^--binding site has yet been described in thermophiles.

Conformational stability of the psychrophilic enzyme

The various structural factors potentially promoting flexibility of *A. haloplanctis* α-amylase (Table 3) occur essentially in the $(\beta/\alpha)_8$ domain A but also affect interactions between the three domains. When compared with the crystal structure of the pancreatic enzyme, the model of the psychrophilic α-amylase is characterized by the lack of 12 surface salt bridges. In most cases, this difference arises from the replacement of the basic residue of the pair by a glutamine residue or an asparagine residue. Weakly polar interactions were analyzed using the angles and interatomic distance parameters given by Burley and Petsko (1988). As shown in Table 3, the number of amino-, oxygen-, and sulfur-aromatic interactions is lower in the bacterial protein. By contrast, the strong conservation of aromatic-aromatic interactions certainly reflects their essential function in the conformation of both enzymes. However, thermophilic enzymes and the thermostable α-amylase from *Bacillus licheniformis* are protected against irreversible thermoinactivation through rigidification of the molecule by additional salt bridges (Perutz and Raidt, 1975; Tomazic and Klibanov, 1988) and weakly polar interactions (Teplyakov et al., 1990).

Amongst the 84 residues forming the hydrophobic clusters of the porcine α-amylase (Raimbaud et al., 1989), 25 subsitutions were noted in the corresponding positions of *A. haloplanctis* α-amylase. 80% of these substitutions are accompanied by a sharp decrease of the hydrophobicity index using either the statistical PRIFT scale or the experimental scale of Aboderin (see Cornette et al., 1987 for normalized values). In addition, 72% of these substitutions increase the main-chain flexibility parameter derived by Karplus and Schultz (1985) from the crystallographic temperature factor of individual amino acids. Assuming that urea and GdmCl act mainly by weakening hydrophobic interactions, their strong denaturing effect on *A. haloplanctis* α-amylase also suggests a low hydrophobicity of the core clusters. Conversely, several studies (Mozhaev et al., 1988), especially a study on the α-amylase of *Bacillus stearothermophilus* (Brosnan et al., 1992) support a reinforcement of hydrophobic interactions in proteins from thermophiles.

The psychrophilic enzyme has the lowest proline content found in α-amylases. The sequence aligment (Fig. 5) shows that 9 proline residues are conserved in both enzymes whereas 12 proline residues are either deleted or substituted by small amino acids such as alanine. These substitutions/deletions mainly occur within loops or turns and favour the flexibility of the chain connecting adjacent secondary structures. Indeed, the thermostability of oligo-1,6-glucosidase from *Bacillus thermoglucosidasius* has been correlated with the presence of additional proline residues (Watanabe et al., 1991) because the

pyrrolidine ring severely restricts the available dihedral angles of the preceding residue and decreases the backbone entropy of unfolding. *A. haloplanctis* α-amylase also possesses a low arginine content. Since the charge resonance of the guanidinium group gives arginine the possibility to form more than one electrostatic bond (Mrabet et al., 1992), an increased arginine content has been correlated with heat stability in thermophilic enzymes (Merkler et al., 1981).

The disulfide bond Cys70-Cys115 is absent in *A. haloplanctis* α-amylase. However, mesophilic α-amylases from *Aspergillus oryzae* (Swift et al., 1991) and *Streptomyces limosus* (Long et al., 1987) are also devoid of this disulfide linkage which does not seem of crucial importance for stability. Negatively charged side chains at the N-terminal first turn of α helices and positively charged side chains at the C-terminal last turn of α helices are considered as stabilizing factors (Shoemaker et al., 1987; Rentier-Delrue et al., 1993). *A. haloplanctis* α-amylase contains less favourable charge-dipole interactions than the porcine enzyme, but unfavourable charge-dipole interactions are numerous in both α-amylases so that no definitive conclusion can be drawn.

In conclusion, the psychophilic enzyme alters several weak interactions in order to gain structural flexibility. Interestingly, enzymes from thermophiles reinforce the same type of interactions indicating that there is a continuum in the strategy of protein adaptation to temperature. One can reasonably assume that the lower conformational stability of *A. haloplanctis* α-amylase ($\approx 10\ kJ \cdot mol^{-1}$) is achieved by the net balance between exothermically formed weak bonds (electrostatic, stabilized by a decrease of temperature) and endothermically formed interactions (hydrophobic, destabilized at low temperature). The determination of the three-dimensional structure of *A. haloplanctis* α-amylase and the construction of site-directed mutants are now required for a detailed analysis of the adaptation parameters suggested by molecular modelling.

This study was supported by the *Fonds de la Recherche Fondamentale et Collective* research contract 2.452692 to C. G. We are also grateful to the *Institut Français de la Recherche Polaire* for generous support and accomodation of research fellows at the antarctic base J-S Dumont d'Urville and to N. Gerardin-Otthiers and R. Marchand for expert technical assistance.

REFERENCES

Bernfeld, P. (1955) Amylases, α and β, *Methods Enzymol. 1*, 149–151.

Brosnan, M. P., Kelly, C. T. & Fogarty, W. M. (1992) Investigation of the mecanisms of irreversible thermoinactivation of *Bacillus stearothermophilus* α-amylase, *Eur. J. Biochem. 203*, 225–231.

Brünger, A. T., Kuriyan, J. & Karplus, M. (1987) Crystallographic R factor refinement by molecular dynamics, *Science 235*, 458–460.

Burley, S. K. & Petsko, G. A. (1988) Weakly polar interactions in proteins, *Adv. Protein Chem. 39*, 125–189.

Cornette, J. L., Cease, K. B., Margalit, H., Spouge, J. L., Berzofsky, J. A. & DeLisi, C. (1987) Hydrophobicity scales and computational techniques for detecting amphipathic structures in proteins, *J. Mol. Biol. 195*, 659–685.

Creighton, T. E. (1991) Stability of folded conformations, *Curr. Opin. Struct. Biol. 1*, 5–16.

Davail, S., Feller, G., Narinx, E. & Gerday, C. (1992) Sequence of the subtilisin-encoding gene from an antarctic psychrotroph *Bacillus* TA41, *Gene (Amst.) 119*, 143–144.

Feller, G., Thiry, M. & Gerday, C. (1991) Nucleotide sequence of the lipase gene *lip2* from the antarctic psychrotroph *Moraxella* TA144 and site-specific mutagenesis of the conserved serine and histidine residues, *DNA Cell Biol. 10*, 381–388.

Feller, G., Lonhienne, T., Deroanne, C., Libioulle, C., Van Beeumen, J. & Gerday, C. (1992) Purification, characterization, and nucleotide sequence of the thermolabile α-amylase from the antarctic psychrotroph *Alteromonas haloplanctis* A23, *J. Biol. Chem. 267*, 5217–5221.

Fontana, A. (1991) How nature engineers protein (thermo)stability, in *Life under extreme conditions: biochemical adaptations* (di Prisco, G., ed.) pp. 89–113, Springer Verlag, Berlin-Heidelberg.

Hochachka, P. W. & Somero, G. N. (1984) *Biochemical adaptations*, Princeton University Press, Princeton, NJ.

Jaenicke, R. (1991) Protein stability and molecular adaptations to extreme conditions, *Eur. J. Biochem. 202*, 715–728.

Karplus, P. A. & Schulz, G. E. (1985) Prediction of chain flexibility in proteins, *Naturwissenschaften 72*, 212–213.

Levitzki, A. & Steer, M. L. (1974) The allosteric activation of mammalian α-amylase by chloride, *Eur. J. Biochem. 41*, 171–180.

Long, C. M., Virolle, M. J., Chang, S. Y., Chang, S. & Bibb, M. J. (1987) α-Amylase gene of *Streptomyces limosus*: nucleotide sequence, expression motifs, and amino acid sequence homology to mammalian and invertabrate α-amylases, *J. Bacteriol. 169*, 5745–5754.

Merkler, D. J., Farrington, G. K. & Wedler, F. C. (1981) Protein thermostability, *Int. J. Pept. Protein Res. 18*, 430–442.

Mozhaev, V. V., Berezin, I. V. & Martinek, K. (1988) Structure-stability relationship in proteins: fundamental tasks and strategy for the development of stabilized enzyme catalysts for biotechnology, *CRC Crit. Rev. Biochem. 23*, 235–281.

Mrabet, N. T., Van den Broeck, A., Van den Brande, I., Stanssens, P., Laroche, Y., Lambeir, A. M., Matthijssens, G., Jenkins, J., Chiadmi, M., Van Tilbeurgh, H., Rey, F., Janin, J., Quax, W. J., Lasters, I., De Mayer, M. & Wodak, S. J. (1992) Arginine residues as stabilizing elements in proteins, *Biochemistry 31*, 2239–2253.

Pace, C. N., Shirley, B. A. & Thomson, J. A. (1989) Measuring the conformational stability of a protein, in *Protein structure, a practical approach* (Creighton, T. E., ed.) pp. 311–330, IRL Press, Oxford.

Perutz, M. F. & Raidt, H. (1975) Stereochemical basis of heat stability in bacterial ferredoxins and in haemoglobin A2, *Nature 255*, 256–259.

Qian, M., Haser, R. & Payan, F. (1993) Structure and molecular model refinement of pig pancreatic α-amylase at 2.1 Å resolution, *J. Mol. Biol. 231*, 785–799.

Raimbaud, E., Buleon, A., Perez, S. & Henrissat, B. (1989) Hydrophobic cluster analysis of the primary sequences of α-amylases, *Int. J. Biol. Macromol. 11*, 217–225.

Raucher, E., Neumann, U., Scaich, E., von Bülow, S. & Wahlefeld, A. W. (1985) Optimized conditions for determining activity concentration of α-amylase in serum, with 1,4-α-D-4-nitrophenylmaltoheptaoside as substrate, *Clin. Chem. 31*, 14–19.

Rentier-Delrue, F., Mande, S. C., Moyens, S., Terpstra, P., Mainfroid, V., Goraj, K., Hol, W. G. J. & Martial, J. A. (1993) Cloning and overexpression of the triosephosphate isomerase genes from psychrophilic and thermophilic bacteria, *J. Mol. Biol. 229*, 85–93.

Robertson, S. P., Potter, J. D. & Rouslin, W. (1982) The Ca^{2+} and Mg^{2+} dependence of Ca^{2+} uptake and respiratory function of porcine heart mitochondria, *J. Biol. Chem. 257*, 1743–1748.

Roussel, A. & Cambillau, C. (1990) Turbo-Frodo, molecular modelling package, in *Silicon graphics geometry partners directory*, p. 109, Silicon Graphics, Montain View, CA.

Shoemaker, K. R., Kim, P. S., York, E. J., Stewart, J. M. & Baldwin, R. L. (1987) Tests of the helix dipole model for the stabilisation of α-helices, *Nature 326*, 563–567.

Swift, H. J., Brady, L., Derewenda, Z. S., Dodson, E. J., Dodson, G. G., Turkenburg, J. P. & Wilkinson, A. J. (1991) Structure and molecular model refinement of *Aspergillus oryzae* (TAKA) α-amylase: an application of the simulated-annealing method, *Acta Crystallogr. B47*, 535–544.

Teplyakov, A. V., Kuranova, I. P., Harutyunyan, E. H., Vainshtein, B. K., Frömmel, C., Höhne, W. E. & Wilson, K. S. (1990) Crystal structure of thermitase at 1.4 Å resolution, *J. Mol. Biol. 214*, 261–279.

Tomazic, S. J. & Klibanov, A. M. (1988) Why is one *Bacillus* α-amylase more resistant against irreversible thermoinactivation than another? *J. Biol. Chem. 263*, 3092–3096.
Ushakov, B. (1964) Thermostability of cells and proteins in poikilotherms, *Physiol Rev. 44*, 518–560
Vihinen, M. & Mäntsälä, P. (1989) Microbial amylolytic enzymes, *Crit. Rev. Biochem. Mol. Biol. 24*, 329–418.
Watanabe, K., Chishiro, K., Kitamura, K. & Suzuki, Y. (1991) Proline residues responsible for thermostability occur with high frequency in the loop regions of an extremely thermostable oligo-1,6-glucosidase from *Bacillus thermoglucosidasius* KP1006, *J. Biol. Chem. 266*, 24287–24294.
Zuber, H. (1988) Temperature adaptation of lactate dehydrogenase. Structural, functional and genetic aspects, *Biophys. Chem. 29*, 171–179.

Supplementary material. **Stability and structural analysis of α-amylase from the antarctic psychrophile *Alteromonas haloplanctis* A23.** Table S1. Salt bridges in *A. haloplanctis* α-amylase and porcine pancreatic α-amylase. Table S2. Aromatic-aromatic interactions in *A. haloplanctis* α-amylase and porcine pancreatic α-amylase. Table S3. Amino-, oxygen-, and sulfur-aromatic interactions in *A. haloplanctis* and porcine pancreatic α-amylases. Table S4. Proline residues in *A. haloplanctis* and porcine pancreatic α-amylases. Table S5. Amino acid substitutions in the hydrophobic clusters of *A. haloplanctis* α-amylase. This information is available, upon request, from the Editorial Office.